

Effect of Lanthanum Content and Substrate Strain on Structural and Electrical Properties of Lead Lanthanum Zirconate Titanate Thin Films

Sheng Tong^{1,2,*}, Manoj Narayanan², Beihai Ma², Shanshan Liu², Rachel E. Koritala³, Uthamalingam Balachandran², and Donglu Shi¹

¹*College of Engineering and Applied Science, University of Cincinnati, Cincinnati, OH 45221, USA*

²*Energy Systems Division, Argonne National Laboratory, Argonne, IL 60439, USA*

³*Materials Science Division, Argonne National Laboratory, Argonne, IL 60439, USA*

Abstract

We investigated the structural, electrical properties of $\text{Pb}_{1-x}\text{La}_x(\text{Zr}_{0.52}\text{Ti}_{0.48})\text{O}_3$ (PLZT) thin films under tensile (Pt/Si) and compressive (LaNiO_3/Ni) strain-states, respectively. The lattice parameter, grain size, remanent polarization of the thin films decreased with increasing La content. For identical compositions, the Curie temperature, remanent polarization, and coercive field were always higher for films on LaNiO_3/Ni than Pt/Si. These suggest that the electrical properties of PLZT thin films can be tuned by altering the dopant level and substrate-induced strain levels.

Key words ferroelectric thin film, thermal strain, lanthanum doping, substrate

* Tel: 01-(630)252-6516; Fax: 01-(630)252-3604; shengtg@mail.uc.edu

The lead lanthanum zirconate titanate, $\text{Pb}_{1-x}\text{La}_x(\text{Zr}_y\text{Ti}_{1-y})\text{O}_3$ (PLZT, $x/y/1-y$) was discovered in 1971 [1,2], and since that time, there has been considerable interest in the development of PLZT-film devices for various applications owing to their excellent ferroelectric and piezoelectric properties. One of the most attractive features of PLZT is that its behavior transitions from normal ferroelectric to relaxor with an increase in La content. Such phase transition can be easily recognized by the change in electrical behavior. For example, the temperature-dependent permittivity peaks would be sharp in normal ferroelectrics and diffuse in relaxors, and the shape of the polarization-electric field (P - E) loops would vary from square to slim [2]. The $\text{Pb}(\text{Zr}_x\text{Ti}_{1-x})\text{O}_3$ (PZT) compositions exhibit exceptional piezoelectric and ferroelectric properties around the morphotropic phase boundary (MPB) with Zr/Ti ratio of 52/48 because the monoclinic Cm phase enhances the possibility of polarization alignments[1,3]. The La donor dopants induce the distortion of unit cells for ease of domain switching and decrease the oxygen vacancies, leading to a higher relative permittivity (ϵ_r), spontaneous polarization (P_s), and lower leakage current [4]. Hence, the PLZT ($x/52/48$) compositions have been well investigated for their advanced dielectric and ferroelectric properties [3,5,6]. As a result of the substrate strain and size effects, the electrical properties and phase transitions of the ferroelectric thin films differ greatly from those of their bulk counterparts. We, therefore, studied the structural and electrical properties of $\text{Pb}_{1-x}\text{La}_x(\text{Zr}_{0.52}\text{Ti}_{0.48})\text{O}_3$ thin films with different La dopant concentrations on silicon and nickel substrates, and compared them to the bulk properties reported in the literature.

Using sol-gel chemistry based on acetic acid, we fabricated PLZT thin films ($x/52/48$, where $x = 0, 1, 3, 5, 10$) on substrates of platinumized silicon (Pt/Si) and of nickel buffered by lanthanum nickel oxide (LaNiO_3 or LNO). The LNO buffer layer is included to avoid nickel

oxidation and diffusion that forms a low-permittivity parasitic layer that contributes to series capacitance. Details on the solution preparation, deposition, and heat treatment conditions are reported elsewhere [7]. The thickness of the platinum bottom electrode on silicon substrate was ~500 nm, and the final thickness of the LNO and PLZT thin films was ~400 nm and ~500 nm, respectively. Platinum top electrodes (250- μm diameter and 100-nm thickness) were deposited through a shadow mask by electron-beam evaporation. The effects of donor dopants and substrates on thin film phases, morphology, dielectric properties and ferroelectric responses were studied by X-ray diffraction (XRD, Bruker AXS diffractometer), field-emission scanning electron microscopy (SEM, Hitachi S4700), LCR meter (Agilent E4980A) using an oscillator level of 0.1 V in conjunction with a Signatone QuieTemp probe station with hot stage (Lucas Signatone Corp., CA), and ferroelectric test system (Radiant Technologies PrecisionPremier II Tester) at 1kHz, respectively.

The θ - 2θ symmetrical reflection XRD measurements were used to characterize the phases of the PLZT thin films. The XRD patterns in Figs. 1(a) and (b) indicate the formation of phase-pure perovskite with pseudo-cubic structure in all PLZT thin films fabricated on both substrates. In Fig. 1(c), the out-of-plane (planes normal to the substrate surface) lattice parameters derived from (002) peaks decrease linearly with increasing La content in which slope of PLZT/LNO/Ni is much larger than that of PLZT/Pt/Si; this behavior is similar to values of c and a of bulk ceramic, respectively [3]. It can be explained by the nature of PLZT thin film strain states and domain structure. The thermal expansion coefficients of the thin film ($\alpha_{\text{PLZT}} = 5.4 \times 10^{-6} \text{ K}^{-1}$) [8] and substrates ($\alpha_{\text{Si}} = 2.6 \times 10^{-6} \text{ K}^{-1}$, $\alpha_{\text{Ni}} = 13.4 \times 10^{-6} \text{ K}^{-1}$) [9] indicate that the PLZT thin films deposited on silicon and nickel substrates are under tensile and compressive stress, respectively [10]. Thus, PLZT/LNO/Ni mainly demonstrates c -domains while a -domains

dominate PLZT/Pt/Si [11,12]. A linear decrease in tetragonality (c/a ratio) of PLZT bulks with increasing La content shows a gradual transition from tetragonal to pseudo-cubic structure, due to the creation of A- and B-site vacancies and the reduction of oxygen vacancies [4]. Same tendency is expected in PLZT thin films, however, due to the 2–3 order differences in the grain sizes between thin films (<100 nm) and bulk ceramic [4,13], the local tetragonality of the thin films cannot directly be characterized. Nonetheless, it is reasonable to consider a higher tetragonality in PLZT/LNO/Ni compared with that of PLZT/Pt/Si based on the fact that the PLZT/LNO/Ni exhibits much larger out-of-plane lattice parameters as shown in Fig. 1(c). [Note that the Pt \(111\) peak in Fig. 1 comes from the top electrode.](#)

Planar SEM images of representative PLZT films doped with 0, 3, and 5 mol% La on both substrates are given in Figs. 2(a)–(f). The morphology of the films was smooth with dense and uniform grains without any obvious secondary phase ([also confirmed by dielectric measurements below](#)). The average surface grain sizes of the PLZT thin films deposited on the Si and Ni substrates were calculated and are shown in [Fig. 2\(j\)](#). Similar to bulk ceramic [14], the surface [grain](#) size of PLZT thin films decreased with the increase of La content in films formed on both substrates. However, the surface grain size of the PLZT thin films was 20–120 nm, which is 2–3 orders lower than that of bulk PLZT ceramic because of different crystallization temperature range [15]. The surface grain size of PLZT/Pt/Si is larger than that of PLZT/LNO/Ni at the same La dopant level. The cross-sectional SEM images of PLZT/Pt/Si shown as insets to [Figs. 2\(g\)-\(i\)](#) exhibit dense and columnar grains. No obvious secondary phases and defects were observed. As shown in [Fig. 2\(j\)](#), the measured thickness of the films is approximately 500 nm and is independent of the La concentration.

The dielectric and ferroelectric properties of PLZT thin films are strongly dependent on the La-dopant level, microstructure, and strain state (tensile or compressive). As shown in Fig. 3, with increasing La content from 0 to 10 mol%, the shape of the P - E loops become slimmer and slanted for PLZT thin films on both Pt/Si and LNO/Ni. The remanent polarization (P_r) and saturation polarization (P_{sat}) also decrease dramatically in PLZT/Pt/Si and PLZT/LNO/Ni with increase in La content. The tetragonality decreases with increasing La content, leading to a reduction in spontaneous polarization in the unit cell. Therefore, the magnitude of the average net polarization in a domain/grain decreases, leading to a reduction in the measured macroscopic P_r and P_{sat} [14,16]. Although the measured P_r is correlated with the unit cell, this is not the case with the coercive electric field (E_c). The macroscopically measured E_c is the “extrinsic” coercive field determined by domain nucleation, dynamic process, which is much lower than the “intrinsic” coercive field that is determined by the free energy profile of the B-site atom in the unit cell [17]. As can be observed in Fig. 3(c), the E_c values of PLZT bulk ceramic and thin films on Pt/Si and LNO/Ni are ~18, ~40, and ~75 kV/cm, respectively. The E_c is almost independent of La content (due to the extrinsic nature of the measured E_c) for the thin film and bulk ceramic, whereas the E_c for thin films is 2-4 times higher than that reported for bulk ceramic [18,19]. The bulk E_c is lower than that of thin films because of grain size effects [16] and depolarization field at or the near electrodes which requires extra charge to compensate the polarization [20,21]. The P - E loops of PLZT/LNO/Ni are “squarer” compared with PLZT/Pt/Si for the same La content. In other words, for an applied field the difference between the P_r and P_{sat} could be small. With an increase of La content from 0 to 10 mol%, the P_r values decrease from ~36 to 20 $\mu\text{C}/\text{cm}^2$ for bulk ceramic, ~23 to 4 $\mu\text{C}/\text{cm}^2$ for thin films on Pt/Si, and ~30 to 11 $\mu\text{C}/\text{cm}^2$ for thin films on LNO/Ni. Although one would expect the P_r of stress-free bulk ceramics in Fig. 3(d) to fall

between that of films under compressive and tensile stress, consideration has to be given to other major factors like grain size, dielectric thickness and depolarization field that plays an important role and influences the measured P_r of bulk ceramics compared to thin films [14,16,20,21]. The thermal strains induced by the thermal expansion mismatch between the substrate and thin film are critical in determining the domain morphology. The c -domain (polarization normal to the surface of the substrate) population and out-of-plane polarization (P_3) decrease with increase in misfit strain from compressive to tensile [12,22,23], resulting in larger P_r in PLZT/LNO/Ni than that in PLZT/Pt/Si [as observed in Fig. 3(d)]. La ions soften the PLZT thin films from normal ferroelectrics into relaxors; however, the substrates partially retain the ferroelectric behavior, especially LNO/Ni substrates. The effect of compressive stress by nickel substrate on PLZT thin films can be compared to “hard” doping in PZT with Fe^{3+} , which limits the domain rotation and results in an increase in P_r and E_c , while the effect of the silicon substrate can be compared to “soft” doping with Nb^{5+} [24].

The effect of La content and substrate on the temperature-dependent permittivity (ϵ_r vs. T) of PLZT thin films is shown in Figs. 4(a) and (b). The temperature corresponding to the permittivity maximum is considered as the Curie temperature (T_c). In general, the room-temperature permittivity was higher for PLZT/Pt/Si compared with PLZT/LNO/Ni for all La concentrations; this substrate effect had been reported previously for PLZT with 8 mol% La [25,26]. In films on Pt/Si (LNO/Ni), the permittivity at room temperature increased from 1370 to 2070 (550 to 980) when La increased from 0 to 3 mol% and decreased to 920 (670) when the La content was further increased to 10 mol%. Similar to PLZT bulk ceramic [3,5,6], the permittivity response was flatter with diffuse phase transition peaks and lower T_c with increasing La content in thin films deposited on PLZT/Pt/Si and PLZT/LNO/Ni, in spite of the notable difference in the

order of phase transition. Bulk ceramics follow first-order phase transition, whereas thin films follow second-order phase transition [18]. This difference is the reason for a sharp increase in the permittivity not being observed at T_c for thin films. The broadening of the ε_r-T curve is caused by factors inherent to the thin films: grain size [13,14], strain effect [27], and the “dead layer” effect [28]. The change in T_c with biaxial stress (compressive/tensile) induced by thermal expansion mismatch is given by the following equation [27,29]:

$$\Delta T_c = 4\varepsilon_0 Q_{12} C \frac{Y}{1-\nu} \Delta\alpha \quad (1)$$

where ΔT_c is the Curie temperature shift, ε_0 is the vacuum permittivity, Q_{12} is the electrostrictive coefficient, Y is the Young’s modulus for PLZT, ν is the Poisson ratio for PLZT, and $\Delta\alpha$ is the thermal coefficient mismatch between substrate (Pt/Si or LNO/Ni) and PLZT thin film [10]. Since Q_{12} is always negative, we concluded that T_c will decrease in the case of tensile stress and vice versa for compressive stress. The change in T_c with increasing La content for PLZT/Pt/Si and PLZT/LNO/Ni along with bulk ceramic is plotted in Fig. 4(c). As predicted by Eq. (1), the T_c for the films under compressive stress (LNO/Ni) is higher, whereas that for the films under tensile stress (Pt/Si) is lower compared with the bulk ceramic. Within the temperature range measured, T_c was observed for PLZT/LNO/Ni with La \geq 8 mol% and PLZT/Pt/Si with La \geq 3 mol%. Although the permittivity shows considerable difference with La content, as seen in Figs. 4(a) and (b), the dielectric loss was \sim 0.05 and did not vary much with increasing La content, temperature, or substrate.

In conclusion, we studied the effects of La content and substrate strain on the structural, ferroelectric, and dielectric properties of PLZT thin films. We found that the lattice parameters, grain sizes, and P_r of PLZT films decreased with increase in La content. The E_c was nearly independent of La content for films. For the same PLZT compositions, the grain size, E_c and

room-temperature ε_r of PLZT/Pt/Si were larger, and the P_r and T_c were lower than those of PLZT/LNO/Ni. These findings indicate that the PLZT electrical properties can be tuned by composition modification and substrate induced strain levels.

Acknowledgement

This work was supported by the U.S. Department of Energy, Vehicle Technologies Program, under Contract DE-AC02-06CH11357. The electron microscopy was carried out at the Electron Microscopy Center for Materials Research at Argonne National Laboratory.

Reference

- [1] G.H. Haertling, *J. Am. Ceram. Soc.* 82 (1999) 797.
- [2] L.E. Cross, in: Walter Heywang, Karl Lubitz and Wolfram Wersing (Ed.), *Piezoelectricity*, 2008, Berlin Heidelberg, 2008, p. 131-155.
- [3] S.M. Gupta, J. Li, D. Viehland, *J. Am. Ceram. Soc.* 81 (1998) 557.
- [4] S. Aggarwal, R. Ramesh, *Annu. Rev. Mater. Sci.* 28 (1998) 463.
- [5] A. Pel áz Barranco, F. Calder ón Pi ñar, O. P érez Mart ínez, *Phys. Stat. Sol. B.* 220 (2000) 591.
- [6] K. Wojcik, J. Błaszczak, J. Handerek, *Ferroelectrics.* 70 (1986) 39.
- [7] B. Ma, S. Tong, M. Narayanan, S. Liu, S. Chao, U. Balachandran, *Mater. Res. Bull.* (2011).
- [8] G.H. Haertling, *J. Am. Ceram. Soc.* 54 (1971) 303.
- [9] R.C. Weast, M.J. Astle, W.H. Beyer, *CRC handbook of chemistry and physics*, CRC press Boca Raton, 1988.
- [10] B. Ma, S. Liu, S. Tong, M. Narayanan, U. Balachandran, *J. Appl. Phys.* 112 (2012) 114117
- [11] G.L. Brennecke, W. Huebner, B.A. Tuttle, P.G. Clem, *J. Am. Ceram. Soc.* 87 (2004) 1459.
- [12] K. Lee, S. Baik, *Annu. Rev. Mater. Res.* 36 (2006) 81.
- [13] Z. Zhao, V. Buscaglia, M. Viviani, M.T. Buscaglia, L. Mitoseriu, A. Testino, M. Nygren, M. Johnsson, P. Nanni, *Phys. Rev. B.* 70 (2004) 024107.
- [14] C.A. Randall, N. Kim, J.P. Kucera, W. Cao, T.R. Shrout, *J Am Ceram Soc.* 81 (1998) 677.
- [15] R.W. Schwartz, *Chem. Mater.* 9 (1997) 2325.
- [16] K. Okazaki, K. Nagata, *J Am Ceram Soc.* 56 (1973) 82.
- [17] S. Ducharme, V.M. Fridkin, A.V. Bune, S. Palto, L. Blinov, N. Petukhova, S. Yudin, *Phys. Rev. Lett.* 84 (2000) 175.
- [18] M. Dawber, K.M. Rabe, J.F. Scott, *Rev. Mod. Phys.* 77 (2005) 1083.
- [19] P.K. Larsen, G.J.M. Dormans, D.J. Taylor, P.J. van Veldhoven, *J. Appl. Phys.* 76 (1994) 2405.
- [20] J. F. M. Cillessen, M. W. J. Prins, and R. M. Wolf, *J. Appl. Phys.*, 81 (1997) 2777.
- [21] C. T. Black, C. Farrel, and T. J. Litaca, *Appl. Phys. Lett.*, 71 (1997) 2041.
- [22] P.E. Janolin, *J. Mater. Sci.* 44 (2009) 5025.
- [23] J. Zhang, D. Schlom, L. Chen, C. Eom, *Appl. Phys. Lett.* 95 (2009) 122904.
- [24] W. Heywang, K. Lubitz, W. Wersing, *Piezoelectricity: Evolution and Future of a Technology*, 2008, Berlin Heidelberg.
- [25] U. Balachandran, D.K. Kwon, M. Narayanan, B. Ma, *J. Eur. Ceram. Soc.* 30 (2010) 365.
- [26] M. Narayanan, B. Ma, S. Tong, R. Koritala, U. Balachandran, *Inter. J. Appl. Ceram. Technol.* (2011).
- [27] S. Tong, M. Narayanan, B. Ma, R. Koritala, S. Liu, U. Balachandran, D. Shi, *Act. Mater.* 59 (2011) 1309.
- [28] M. Stengel, N.A. Spaldin, *Nature.* 443 (2006) 679.
- [29] G. Catalan, M. Corbett, R. Bowman, J. Gregg, *J. Appl. Phys.* 91 (2002) 2295.

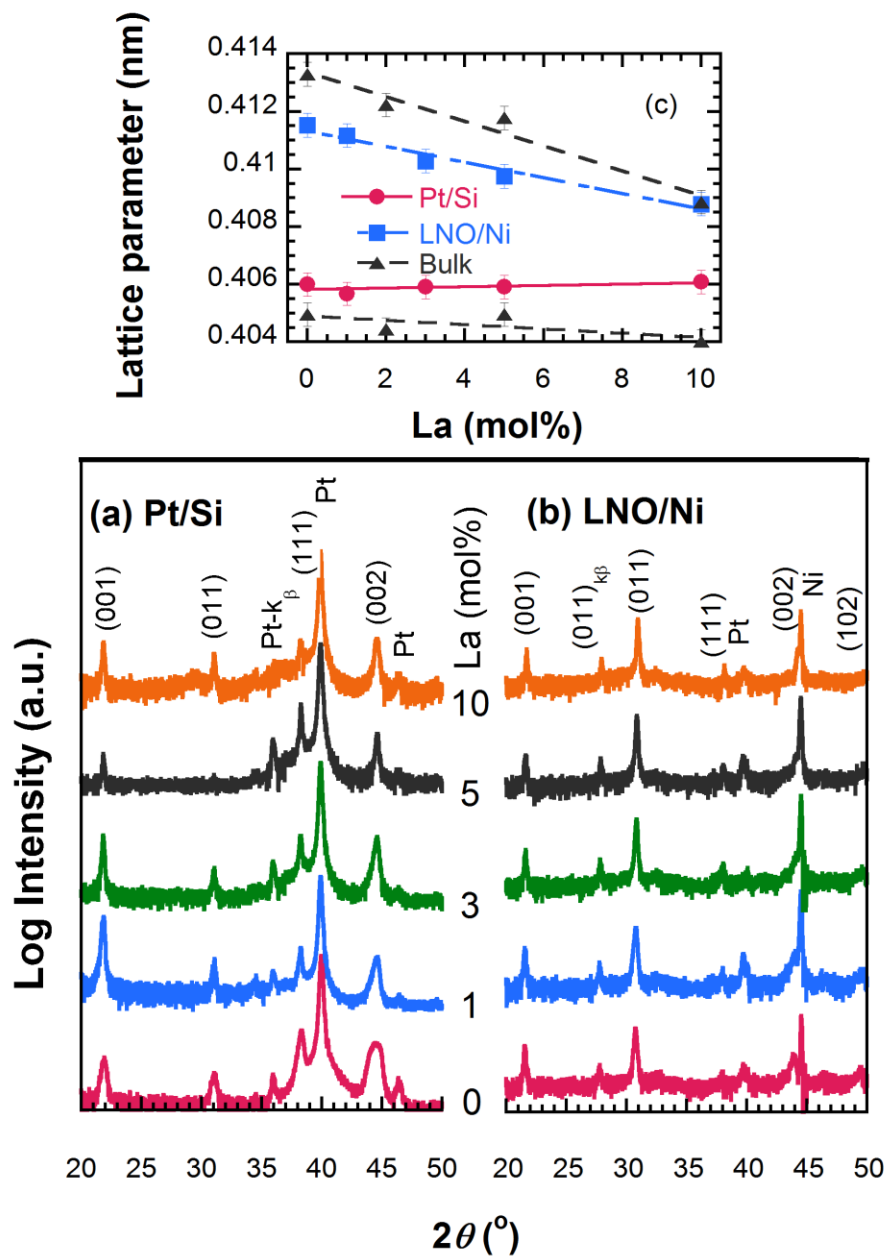


Fig. 1 XRD patterns of PLZT thin films deposited on Pt/Si (a) and LNO/Ni (b) substrates. (c) Lattice parameters of PLZT thin films and bulk as function of La content. (Data for bulk ceramic from Ref. [3])

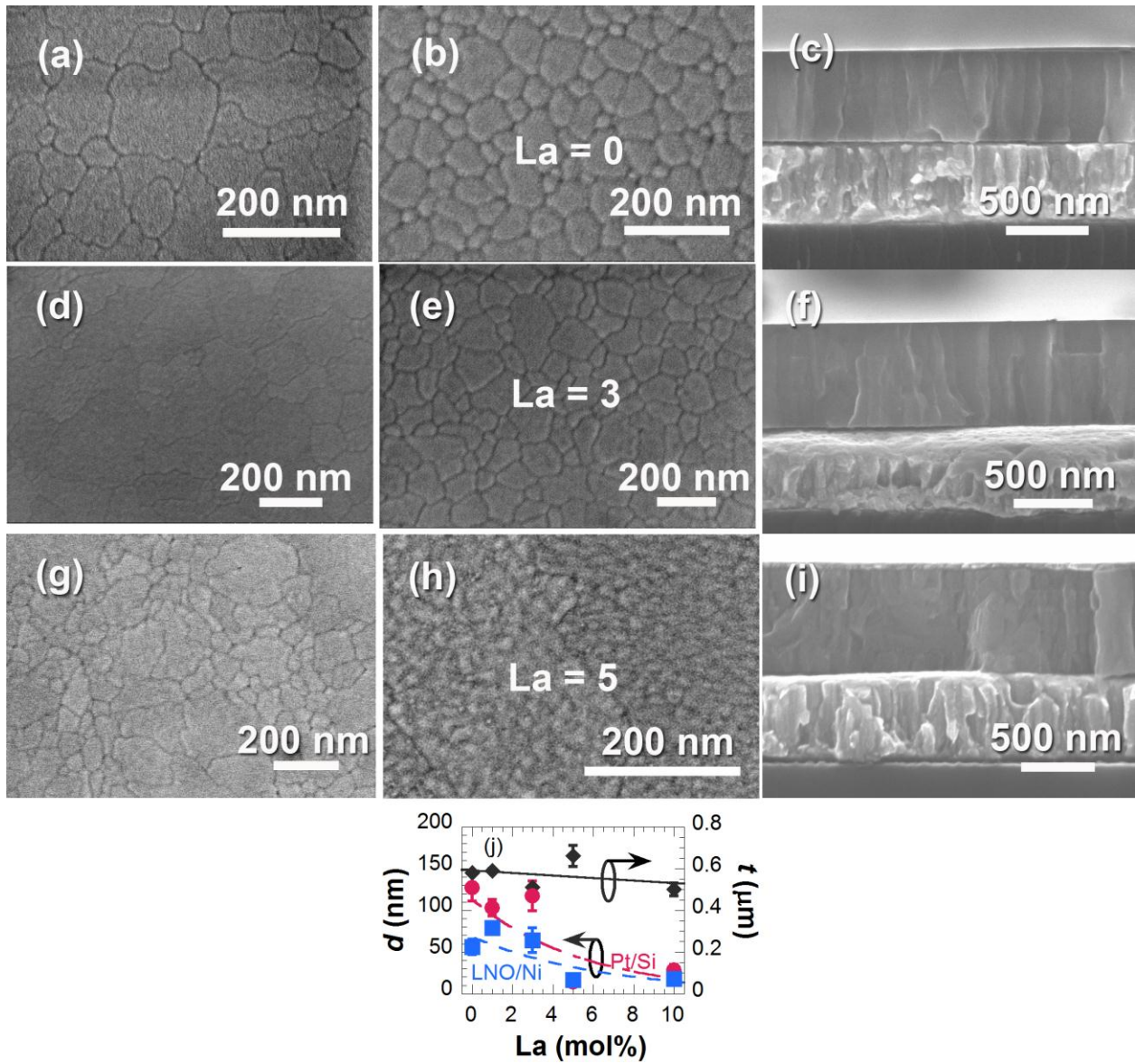


Fig. 2 SEM micrographs of PLZT (La content of 0, 3, and 5 mol%) thin films deposited on Pt/Si (planar: a, d, g; cross-sectional: c, f, i) and LNO/Ni (b, e, h). (j) Grain size d and thickness t as a function of La content.

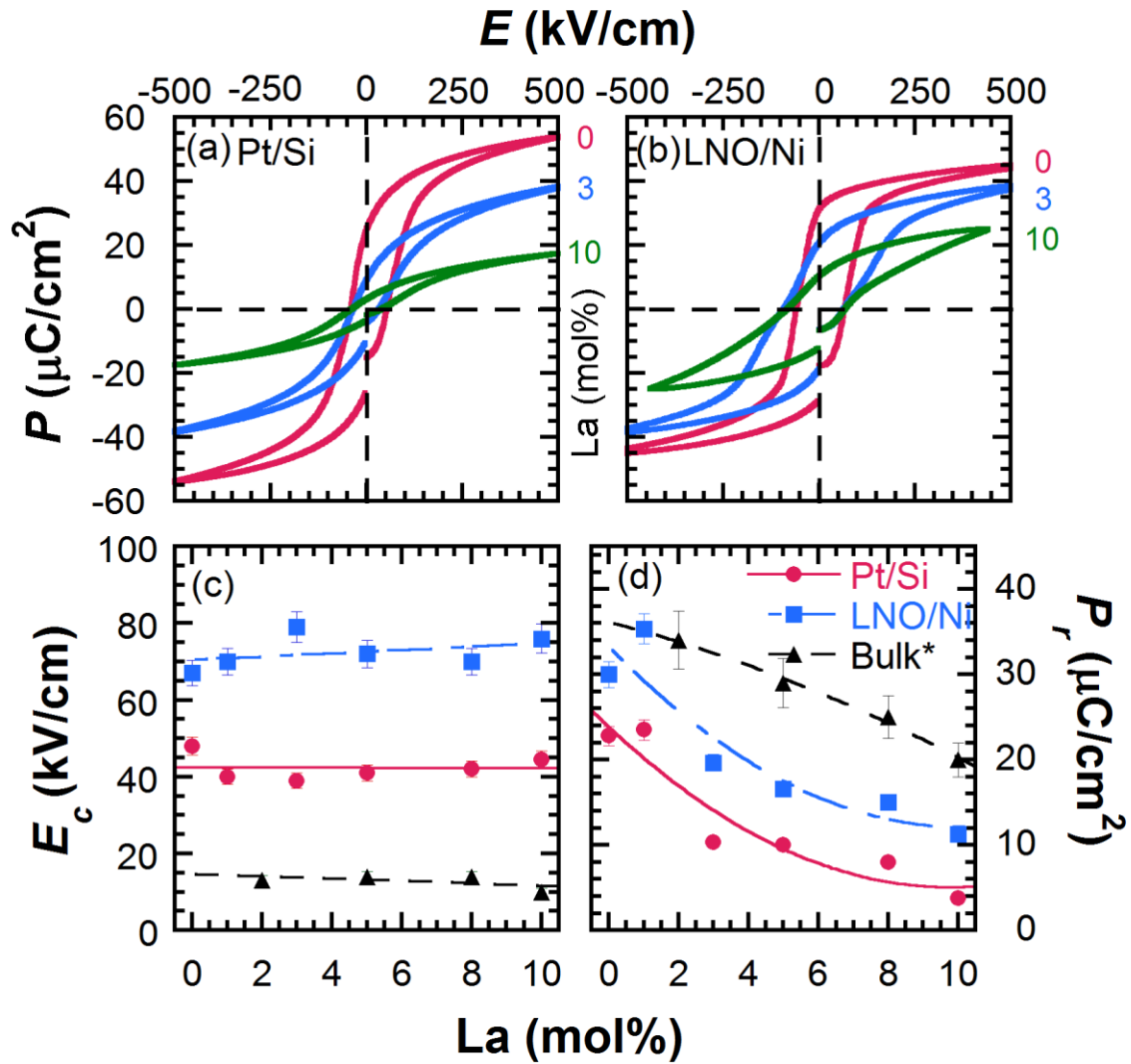


Fig. 3 Hysteresis loops of PLZT (La = 0, 3, and 10 mol%) thin films deposited on Pt/Si (a) and LNO/Ni (b). E_c (c) and P_r (d) of PLZT as a function of La content for PLZT thin films and bulk ceramic. *Ref. [3].

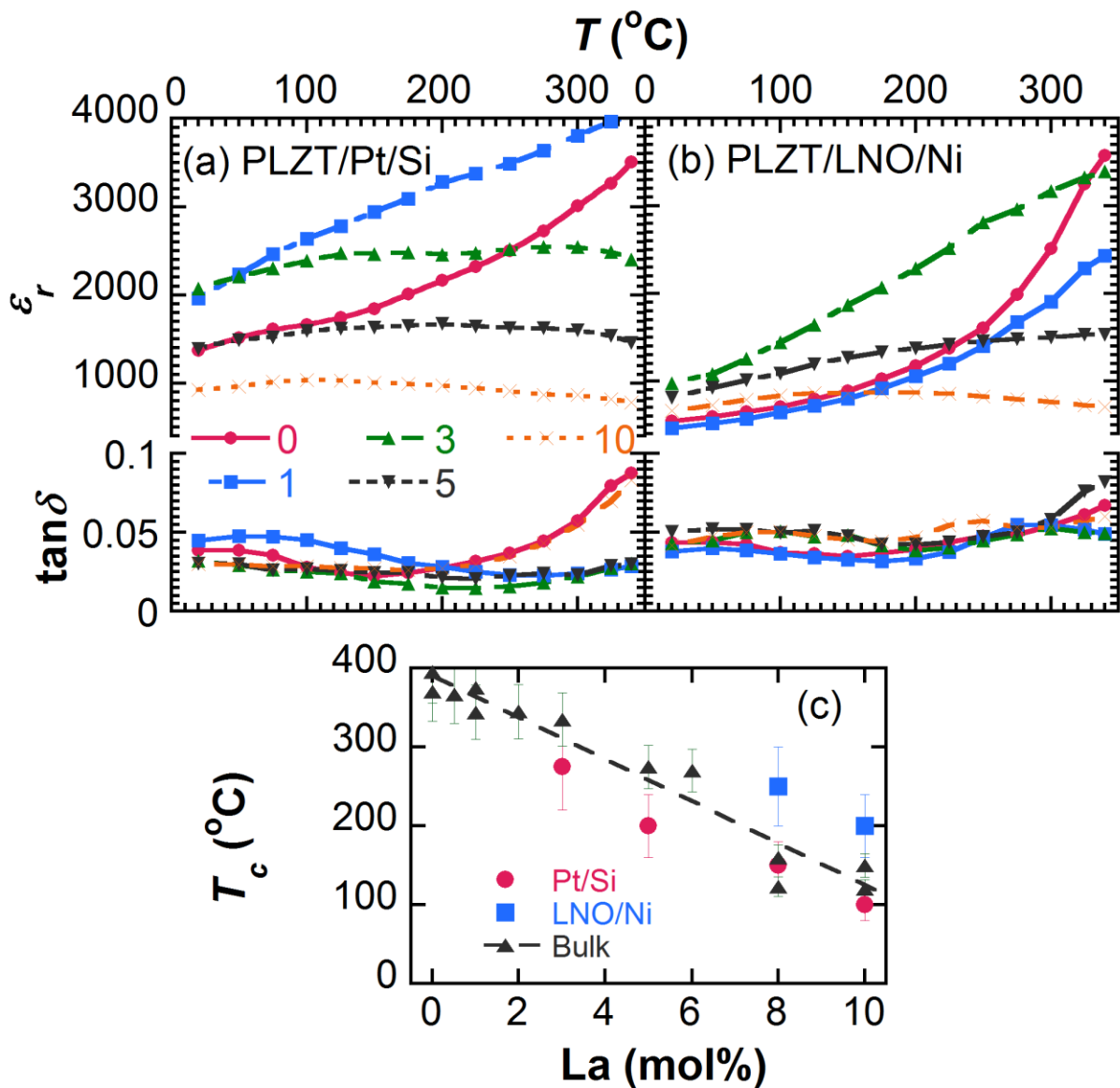


Fig. 4 Temperature-dependent dielectric properties of PLZT (La content of 0-10 mol%) thin films deposited on (a) Pt/Si and (b) LNO/Ni substrates at 10 kHz. (c) T_c of PLZT as a function of La content. The line is obtained by fitting the T_c data for PLZT bulk ceramic. The T_c values for PLZT bulk ceramic and PLZT (8/52/48) thin films were taken from Refs. [3,5,6] and [7,25], respectively.